ISSN 1 746-7233, England, UK
World Journal of Modelling and Simulation
Vol. 12 (2016) No. 4, pp. 268-279

Effect of hall and ion slip on peristaltic blood flow of Eyring Powell fluid in a non-uniform porous channel

M. M. Bhatti[1], M. Ali Abbas[2*], M. M. Rashidi[3,4]

[1] Shanghai Institute of Applied Mathematics and Mechanics, Shanghai University, Shanghai 200072, China
[2] Department of Mathematics, Shanghai University, Shanghai 200444, China
[3] Shanghai Key Lab of Vehicle Aerodynamics and Vehicle Thermal Management Systems, Tongji University, Shanghai 201804, China
[4] ENN-Tongji Clean Energy Institute of advanced studies, Shanghai 200072, China

(*Received March 16 2016, Accepted June 27 2015*)

Abstract. The effect of hall and ion slip on peristaltic blood flow of Eyring Powell in a non-Uniform Porous two-dimensional channel has been studied under the approximation of long wavelength and zero Reynolds number (creeping flow regime). The mathematical modelling of the governing flow problem is obtained with the help of Ohm's law and momentum equation. The resulting non-linear partial differential equation is solved with the help of a perturbation method. The analytic and numerical results of different parameters are demonstrated mathematically and graphically. The present analysis is also applicable for three dimension channels with their respective modifications and assumptions. It is observed that pressure tends to rise due to the influence of Hartmann number but its attitude is opposite for Hall and Ion slip effect. Comparison between Newtonian and non-Newtonian fluid have also presented with the help of tables. This present investigation is also applicable in various biomedical, pharmacological engineering and peristaltic pumping.

Keywords: Blood flow, Ohm's Law, non-Newtonian fluid, Porous medium

1 Introduction

A phenomenon in which reduction and expansion of an extensible tube generate dynamic waves which propagate along the length of the tube infusing and transporting the fluid in the direction of wave propagation is known as peristaltic flow. Some certain physical phenomena, like a movement of Chyme in the gastrointestinal tract, transport of urine from a kidney to bladder through the ureter, the movement of spermatozoa in the ducts efferent ducts of male reproduction tract, Venules and capillaries involve peristaltic motion. Peristaltic pumping also appears in many practical applications such as finger and roller pumps which are frequently used for pumps corrosive fluids. A theoretical analysis of the peristaltic flow in the range of balanced Reynolds number is utmost difficult because of the non-linearity owing in the interaction between moving wall and the flow field. Numerous investigation of peristaltic flow with analytic and numerical results with different geometrical aspects had been reported by a number of researchers. Fung and Yih[8] first studied a peristaltic flow with mild non-linear effects and a small ratio of amplitude to wavelength. Shapiro et al.[14] investigated the peristaltic pumping with long wavelength and low Reynolds number. He described theoretically for both axisymmetric and plane geometries whose range lies from 0 to 1. He also analysed that pressure rise is decreasing linearly per wavelength with increasing time mean flow.

Flow through a porous medium is very helpful in separating particles from the fluid. Particles that are very bigger than the size of the pores that binds to the boundary of the walls. Basically, a porous medium is a material volume that contains solid matrix with an interconnected void. Porosity means the ratio between

* Corresponding author. *E-mail address*: muhammad09@shu.edu.cn; mubashirme@yahoo.com

the volume void space and the total volume of the medium. It is important to note that porous medium is characterised not only by its porosity but also the measure of flow conductivity in the porous medium that is called permeability. In different biological organs and tissues, the role of porous media plays a vital role. Rajagopal and Gupta[22] found the exact solution for the flow of non-Newtonian fluid past an infinite porous plate. Later, Rajagopal et al.[41] also presented the existence theorem with the help of shooting method for in-compressible third-grade fluid past a porous infinite plate having suction at the plate. He applied numerical method instead of perturbation method due its rapid convergence. Srinivas and Gayathri[47] investigated the Peristaltic flow of Newtonian fluid under the effects of heat and mass transfer in the porous asymmetric channel. He described the analytic solution for the temperature, axial velocity, stream function and pressure gradient, whereas trapping phenomena and shear stress was analysed numerically. Some more literature on the present topic is available in [1, 5, 6, 25, 39] and several therein.

In most of the theoretical and experimental observations, it is found that the blood and the others biological and physiological fluids act like a non-Newtonian fluid[18, 20, 21, 46, 48]. However, this analysis gives a suitable understanding of peristaltic flow in the ureter, but it gives unsatisfactory results when peristaltic phenomena are found in small blood vessels, intestine and lymphatic vessels. There are three types of functions that blood performs in the body i.e., regulation of the bulk equilibria, transport throughout the body and body immune defence against various bodies. It gives oxygen, energy and provides different types of nutrients such as glucose, amino acids, provides, vitamins, glucids and mineral ions to the tissues and eliminates carbon dioxide and different waste products of cell metabolism through lungs and purifies various organs. Srivastava et al.[42] investigated the peristaltic transport of Newtonian and non-Newtonian physiological fluids in non-uniform geometries. It has now cleared that many of the physiological fluids act like a non-Newtonian fluid. Mekheimer[16] studied the peristaltic blood flow of couple stress in a non-uniform geometry under the effects of a magnetic field. The peristaltic flow of Newtonian fluid in geometry with the uniform cross section is not applicable while explaining the phenomena of transferring the fluid in different biological systems.

MHD (Magnetohydrodynamic) peristaltic flow in different geometries with elastic, rhythmically contracting walls is of interest in contact with certain problems of the movement of physiological conductive fluids. The basic perception regarding MHD is the magnetic field which induces the currents in conductive moving fluids which in results generates the forces on the fluid and also varies the magnetic field itself. It is well known that when any conductor comes into a magnetic field which in results creates a voltage, which is perpendicular to the current and field, this effect is known as Hall Effect. With the help of Hall Effect, the velocity of the fluid can also be measured. Gad[9] found the effects of hall current on peristaltic transport having flexible walls. He observed that the mechanism of "mean flow reversal" is existing at the boundaries of the channel and at the centre of the channel. He also observed that when the wall damping and hall parameter increases then flow reversal increases whereas it reduces when the Hartman number and the wall tension increases. Stud et al.[44] examined the impact of moving magnetic field on blood flow and they analysed that impact of the magnetic field increases the velocity of the blood. Agarwal and Anwar Uddin[2] examined the effects of magnetic field on blood flow by considering a suitable and simple mathematical model. He analysed that blood flow in different arteries with arterial diseases such as arterial stenos or arteriosclerosis, the impact of a magnetic field can be employed as blood pump in achieving cardiac operations. Several Investigations are obtained with different Newtonian and non-Newtonian fluids can be found from refs[7, 10–13, 15, 17, 23, 26–28, 30, 35–38, 40, 43, 45].

With the above discussion in mind, the purpose of this present study is to analyse the effects of a hall and Ion slip on peristaltic flow of non-Newtonian Eyring Powell fluid through a non-uniform porous channel. A motivation in the present study is that such analysis of hydro-magnetic Eyring Powell fluid is very helpful in understanding the mechanism of peristaltic muscular contraction and expansion in moving the electrically conducting biological fluids, besides it has a huge application to the other bio-medical engineering and physiological problems. Various problems that deal with MHD flow through a porous medium with Hall current play a vital role in controlling the temperature of blood. The governing flow problem is modelled with the help long wavelength and creeping flow regime. The resulting nonlinear differential equation are solved with the help of perturbation method[3, 4, 19, 24, 29, 31–34]. The impact of all the emerging parameters are discussed with the help of graphs and tables.

2 Mathematical formulation

Let us suppose the unsteady irrotational, hydromagnetic flow of Eyring Powell fluid, which is incompressible and electrically conducting by an external magnetic field B is applied through a two-dimensional non-uniform channel having sinusoidal wave moving down towards its porous walls. We have selected a Cartesian coordinate system for the channel in such a way that x-axis is taken along the axial direction and y-axis is taken along the transverse direction. The geometry of the governing flow problem can be described as

$$h(\tilde{x},\tilde{t}) = b(\tilde{x}) + \tilde{a}\sin\frac{2\pi}{\lambda}(\tilde{x}-\tilde{c}\tilde{t}), \tag{1}$$

where $b(\tilde{x}) = b_0 + \tilde{x}$.

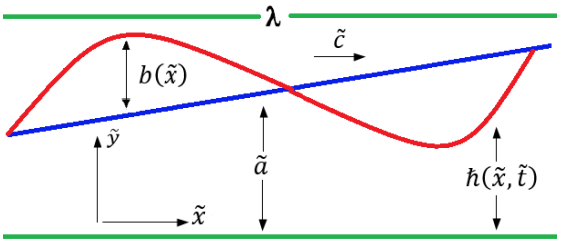

Fig. 1: Geometry of the problem

Let $(\tilde{u},\tilde{v},0)$ be the velocity for the flow in a non-uniform channel. The generalized for of ohm's law with hall and ion-slip effect can be written as [9]

$$j = \sigma(E + V\times B) - \frac{\omega_e\tau_e}{B}(j\times B) - \frac{\omega_e\tau_e\beta_i}{B^2}[(j\times B)\times B]. \tag{2}$$

Solving Eq. (2)we get

$$j_{\tilde{x}} = \frac{\sigma[(1+\beta_e\beta_i)(E_{\tilde{x}} - B\tilde{v}) + \beta_e(E_{\tilde{y}} + B\tilde{u})]}{(1+\beta_e\beta_i)^2 + \beta_e^2}, \tag{3}$$

and

$$j_{\tilde{y}} = \frac{\sigma[(1+\beta_e\beta_i)(E_{\tilde{y}} - B\tilde{u}) + \beta_e(E_{\tilde{x}} + B\tilde{v})]}{(1+\beta_e\beta_i)^2 + \beta_e^2}, (4) \tag{4}$$

where $\beta_e = \omega_e\tau_e$. With the help of Darcy and ohms Law, the continuity equation and momentum equation for the governing flow problem of an Eyring Powell fluid can be written as

$$\frac{\partial\tilde{u}}{\partial\tilde{x}} + \frac{\partial\tilde{v}}{\partial\tilde{y}} = 0, \tag{5}$$

$$\rho\left(\frac{\partial\tilde{u}}{\partial\tilde{t}} + \tilde{u}\frac{\partial\tilde{u}}{\partial\tilde{x}} + \tilde{v}\frac{\partial\tilde{u}}{\partial\tilde{y}}\right) = -\frac{\partial\tilde{p}}{\partial\tilde{x}} + \frac{\partial S_{\tilde{x}\tilde{x}}}{\partial\tilde{x}} + \frac{\partial S_{\tilde{x}\tilde{y}}}{\partial\tilde{y}} + j_{\tilde{x}}\times B - \frac{\mu}{k_1}\tilde{u}, \tag{6}$$

$$\rho\left(\frac{\partial\tilde{v}}{\partial\tilde{t}} + \tilde{u}\frac{\partial\tilde{v}}{\partial\tilde{x}} + \tilde{v}\frac{\partial\tilde{v}}{\partial\tilde{y}}\right) = -\frac{\partial\tilde{p}}{\partial\tilde{y}} + \frac{\partial S_{y\partial\tilde{x}}}{\partial\tilde{x}} + \frac{\partial S_{\tilde{y}\tilde{y}}}{\partial\tilde{y}} + j_{\tilde{y}}\times B - \frac{\mu}{k_1}\tilde{v}. \tag{7}$$

The stress tensor of the Eyring Powell fluid which is defined as [25]

$$S = \mu\nabla V + \frac{1}{B}\sinh^{-1}\left(\frac{\nabla V}{C}\right). \tag{8}$$

It is now convenient to define the non-dimensional quantities

$$
\begin{aligned}
&x=\frac{\tilde{x}}{\tilde{\lambda}}, y=\frac{\tilde{y}}{b_0}, t=\frac{\tilde{c}\tilde{t}}{\tilde{\lambda}}, u=\frac{\tilde{u}}{\tilde{c}}, v=\frac{\tilde{v}}{(\tilde{c}\delta)}, p=\frac{\tilde{p}b_0^2}{\lambda\mu\tilde{c}},\\
&h=\frac{\hbar}{b_0}, \Phi=\frac{\tilde{a}}{b_0}, Re=\frac{\tilde{c}\rho\tilde{a}}{\mu}, \delta=\frac{\tilde{a}}{\tilde{\lambda}}, \alpha_1=\frac{1}{\mu BC},\\
&M=\frac{\tilde{c}_1^2}{6\tilde{a}C^2}, M=(\frac{B^2a^2\sigma}{\mu})^{1/2}, k=\frac{k_1^2}{\tilde{a}^2}, v=\frac{\tilde{v}\tilde{a}\tilde{c}}{\lambda}.
\end{aligned}
\tag{9}
$$

Using the above non-dimensional quantities in Eq. (5) to Eq. (7), after dropping the tilde, we get

$$
\frac{\partial u}{\partial x}+\frac{\partial v}{\partial y}=0, \tag{10}
$$

$$
\begin{aligned}
\mathrm{Re}\delta\left(\frac{\partial u}{\partial t}+u\frac{\partial u}{\partial x}+v\frac{\partial u}{\partial y}\right)&=-\frac{\partial p}{\partial x}+\frac{\partial S_{xx}}{\partial x}+\frac{\partial S_{xy}}{\partial y}\\
&\quad-M^2\left(\frac{[(1+\beta_e\beta_i)u+\beta_e\delta v]}{(1+\beta_e\beta_i)^2+\beta_e^2}\right)-\frac{u}{k},
\end{aligned}
\tag{11}
$$

$$
\begin{aligned}
\mathrm{Re}\delta^3\left(\frac{\partial v}{\partial t}+u\frac{\partial v}{\partial x}+v\frac{\partial v}{\partial y}\right)&=-\frac{\partial p}{\partial y}+\delta\frac{\partial S_{yx}}{\partial x}+\delta\frac{\partial S_{yy}}{\partial y}\\
&\quad-\delta M^2\left(\frac{[-(1+\beta_e\beta_i)\delta v+\beta_e\delta u]}{(1+\beta_e\beta_i)^2+\beta_e^2}\right)-\frac{\delta v}{k},
\end{aligned}
\tag{12}
$$

where

$$
S_{xx}=\delta\frac{\partial u}{\partial x}+\left(\frac{\delta}{\alpha_1}\frac{\partial u}{\partial x}-\delta^3M\left(\frac{\partial u}{\partial x}\right)^3\right), S_{xy}=S_{yx}=\frac{\partial u}{\partial y}+\left(\frac{1}{\alpha_1}\frac{\partial u}{\partial y}-M(\frac{\partial u}{\partial y})^3\right). \tag{13}
$$

Let us consider the assumptions of long wavelength and low Reynolds number, then Eq. (10) to Eq. (12) takes the new form

$$
-\frac{\partial p}{\partial x}+\left(1+\frac{1}{\alpha_1}\right)\frac{(\partial^2u)}{\partial y^2}-M\left(\frac{\partial}{\partial y}\left(\frac{\partial u}{\partial y}\right)^3\right)-M^2(\frac{(1+\beta_e\beta_i)u}{(1+\beta_e\beta_i)^2+\beta_e^2})-\frac{u}{k}=0, \tag{14}
$$

and their respective boundary conditions are

$$
u'(0)=0 \text{ and } u(h)=0, \tag{15}
$$

where $h=1+\frac{\lambda x}{\tilde{a}}+\phi\sin 2\pi(x-t)$ and $\Phi=\frac{b}{\tilde{a}}<1$.

3 Method of solution

The Homotopy perturbation method for the non-linear partial differential Eq. (13) can be defined as [19]

$$
\begin{aligned}
h(w,q)=&(1-q)(L(w)-L(\tilde{w}_0))+q\left(L(w)-\frac{\partial p}{\partial x}-M(\frac{\partial}{\partial y}(\frac{\partial w}{\partial y})^3\right)\\
&-M^2\left(\frac{(1+\beta_e\beta_i)w}{(1+\beta_e\beta_i)^2+\beta_e^2})-\frac{w}{k}\right),
\end{aligned}
\tag{16}
$$

Here, L describes the linear operator and we have selected the following linear operator as

$$
L=(1+\frac{1}{\alpha_1})\frac{\partial^2}{\partial y^2}. \tag{17}
$$

We have selected the following initial guess as

$$\tilde{w}_0 = \frac{(y-h)(y+h)}{(1+1/\alpha_1)}. \tag{18}$$

Let us define

$$w(x,y) = w_0 + qw_1 + q^2 w_2 + \cdots . \tag{19}$$

With the help of Eq. (19) and Eq. (16) and then comparing powers of q, we can easily found the system of equations with their relevant boundary conditions. According to the methodology of HPM, we found the final solution as $(q \to 1)$ which is found as

$$u(x,y) = w(x,y)_{q\to 1} = w_0 + w_1 + w_2 + \cdots . \tag{20}$$

The resulting solutions for velocity are evaluated using Eq. (18) and it can be written as

$$\begin{aligned} u(x,y) =& \frac{\alpha_1(y-h)(y+h)}{1+\alpha_1} - \frac{1}{12(1+\alpha_1)^4(1+\beta_e(\beta_e+2\beta_i+\beta_e\beta_i^2))k} \\ & \alpha_1^2(h-y)(h+y)(h^2(-5(1+\alpha_1)^2(1+kM^2+\beta_e(\beta_e+2\beta_i+\beta_e\beta_i^2+\beta_i kM^2)) \\ & + 24\alpha_1^2(1+be(\beta_e+2\beta_i+\beta_e\beta_i^2))kM) + 6(1+\alpha_1)^2(1+\beta_e(\beta_e+2\beta_i+\beta_e\beta_i^2)) \\ & k(-4+\frac{dp}{dx}) + (1+\alpha_1)^2(1+\beta_e(\beta_e+2\beta_i+\beta_e\beta_i^2))y^2 + k((1+\alpha_1)^2(1+\beta_e\beta_i)M^2 \\ & + 24\alpha_1^2(1+\beta_e(\beta_e+2\beta_i+\beta_e\beta_i^2))M)y^2). \end{aligned} \tag{21}$$

The instantaneous volume rate $Q(x,t)$ can be written as

$$Q(x,t) = \int_0^h u(x,y)dy. \tag{22}$$

The pressure gradient can be calculated from the above expression and after some simplification it can be written as

$$\begin{aligned} \frac{dp}{dx} =& \frac{(3(1+\alpha_1)^2)}{\alpha_1^2 h^3}\left[\frac{4\alpha_1^2 h^3}{3(1+\alpha_1)^2} - \frac{2\alpha_1 h^3}{3+3\alpha_1}\right. \\ & \left. + \frac{4\alpha_1^2 h^5((1+\alpha_1)^2}{15(1+a1)^4}\left(\frac{1}{k} + \frac{(1+\beta_e\beta_i)M^2}{1+\beta_e(\beta_e+2\beta_i+\beta_e\beta_i^2)} - 6\alpha_1^2 M\right) - Q\right]. \end{aligned} \tag{23}$$

The Pressure rise (ΔP_L) and the Friction force (ΔF_L) at the wall in the non-uniform channel of length "L" are evaluated numerically and it can be defined in their non-dimensional form as [1, 16]

$$\Delta P_L = \int_0^{L/\lambda} \frac{dp}{dx}dx, \tag{24}$$

$$\Delta F_L = \int_0^{L/\lambda} (-h\frac{dp}{dx})dx. \tag{25}$$

4 Numerical results and discussion

In this section influence of different parameters of interest are investigated by graphically. To discuss the above results more vigorously, we assume that for instantaneous volume flow rate $Q(x,t)$ is periodic and is defined by

$$Q(x,t) = \bar{Q} + \phi \sin 2\pi(x-t), \tag{26}$$

where $\bar{Q}$ describes the average time flow over one period of the wave. With the help of this form $Q(x,t)$, we will numerically compute the expression of pressure rise (ΔP_L), Friction force (ΔF_L) over the length (L) of the non-uniform channel for different values of fluid parameter (α_1, M), Hartman number (M), Hall parameter (β_e), Ion slip parameter (β_i), porosity parameter k and average time flow rate $(\bar{Q})$. The values that are used for the graphical demonstration is $= 5 \times 10^{-5}$, $L = \lambda = 10$ cm and $b_0 = 1 \times 10^{-2}$ cm. Furthermore, In Eq. (13) by taking $(\alpha_1, k) \to \infty$, $(M, M) = 0$, the present results can be achieved to the results obtained by Shapiro et al.[26] and Srivastava and Srivastava[43] for a Newtonian fluid case (Power Law index $n = 1$). Moreover, Eq. (13) can also reduce to the same results obtained by Gupta and Seshadri[10] by taking $(\alpha_1, k) \to \infty$, $(M, M) = 0$. The present analysis can also be reduce to the similar results obtained by Mekheimer[16] for Newtonian fluid (couple stress parameter $\gamma \to \infty$) by taking $(\alpha_1, k) \to \infty, (M = 0)$. Tab. 1 shows the comparison of pressure rise and friction forces for various values amplitude ratio. Tab. 2 shows the numerical comparison between Newtonian $(\alpha_1, M) \to (\infty, 0)$ and non-Newtonian fluid $(\alpha_1, M) \neq (\infty, 0)$.

In bio-medical engineering, blood pulse can be measure with the help of Hall Effect. A magnetic field is applied on the body to generate the blood polarization. Due to the applied magnetic field on the skin, a magnetic signal is received from electrodes in the blood. Unfortunately, this technique is not suitable due to its interference and noise which rely on better electrical touch of the electrodes on the skin. It can be observed from Fig. 2(a) that when the fluid parameter (α_1), increases then the pressure rise increases. It depicts from Fig. 2(b) that when the hall effect parameter (β_e) increases then the pressure rise tends to diminishes and the same behaviour has keenly been observed for the Ion slip parameter (β_i) in Fig. 3(a). It can be seen from Fig. 3(b) that the greater influence of porosity parameter leads to decrease the pressure rise. From Fig. 4 it is concluded that in the presence of magnetic field, pressure rise increases. It is due to fact that in the presence of magnetic field, a Lorentz force originated which opposes the flow and hence, greater pressure is required to pass through it.

The maximum pressure rise $\Delta P_{\max}$ is obtained by putting $\tilde{Q} = 0$ in Eq. (25). Fig. 5 to Fig. 6 is plotted against Hartman number (M) for various values of Hall parameter (β_e), Ion slip parameter (β_i) and porosity parameter (k). It can be observe from Fig. 5 that with the increment in Hall parameter (β_e), maximum pressure rise decreases and same behavior has been analysed for Ion slip parameter (β_i) in Fig. 6(a). It can easily noticed from Fig. 6(b) that maximum pressure rise decreases when the porosity parameter (k) increases. Fig. 7 to Fig. 8 is plotted for Friction force F_L for various values of Hall parameter (β_e), Ion slip parameter (β_i), porosity parameter (k) and Hartman number (M). It can be seen from all these figures that Friction forces have opposite behaviour as compared to pressure rise. Fig. 9 and Fig. 10 have been prepared for pressure rise versus average volume flow rate $\bar{Q}$. It can easily be seen from these figures that pressure rise decreases when (β_e), (β_i) and (k) increases. This present investigation is also applicable in different drug delivery systems in biological, pharmacological engineering and peristaltic pumping.

Table 1: Comparison of numerical results for pressure rise (ΔP_L) and friction force (ΔF_L) for different values of amplitude ratio (ϕ)

Q	ΔP_L for $\phi = 0.2$	ΔP_L for $\phi = 0.3$	ΔF_L for $\phi = 0.2$	ΔF_L for $\phi = 0.3$
0	−3.1593	−1.2940	3.6196	1.7254
0.1	−3.1501	−1.3649	3.3320	1.3435
0.2	−2.5401	0.0416	2.2307	−0.5420
0.3	−1.6201	2.3435	0.7724	−3.1656
0.4	−1.1515	3.1935	−0.2719	−4.8269
0.5	−1.2675	2.6095	−0.5192	−5.0137
0.6	−1.6277	1.7082	−0.0372	−4.1209
0.7	−2.0322	0.8663	0.9490	−2.5308
0.8	−2.4420	0.0863	2.1289	−0.6775
0.9	−2.8441	−0.6587	3.1336	0.9055
1.0	−3.1593	−1.2940	3.6196	1.7254

Table 2: Numerical comparison for velocity profile between Newtonian and non-Newtonian fluid

h	u (Newtonian fluid)	u (non-Newtonian fluid)	u (non-Newtonian fluid)	u (non-Newtonian fluid)
0	0.4499	0.5592	0.5625	0.5659
0.1367	0.4490	0.5527	0.5557	0.5589
0.2735	0.4459	0.5332	0.5357	0.5383
0.4103	0.4400	0.5011	0.5028	0.5045
0.5470	0.4299	0.4570	0.4576	0.4581
0.6838	0.4136	0.4017	0.4011	0.4004
0.8206	0.3872	0.3361	0.3344	0.3327
0.9573	0.3451	0.2616	0.2592	0.2566
1.0941	0.2779	0.1795	0.1769	0.1743
1.2309	0.1707	0.0917	0.0898	0.0878
1.3677	0	0	0	0

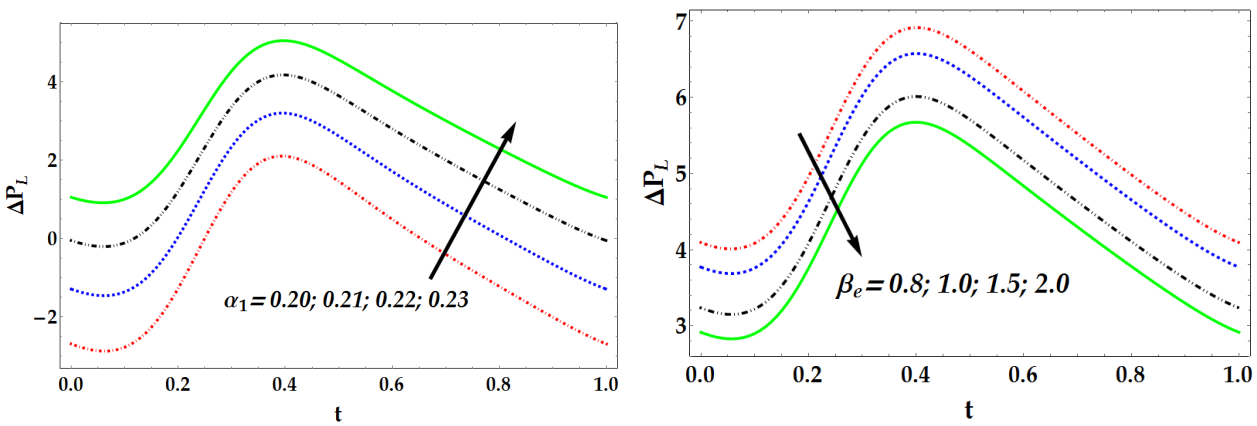

(a) (b)

Fig. 2: Pressure rise for various values of α_1 and β_e. For fixed $(\bar{Q}) = 0.25$, $M = 0.1$, $M = 2$, $\phi = 0.3$, $k = 0.1$, $\beta_i = 1$

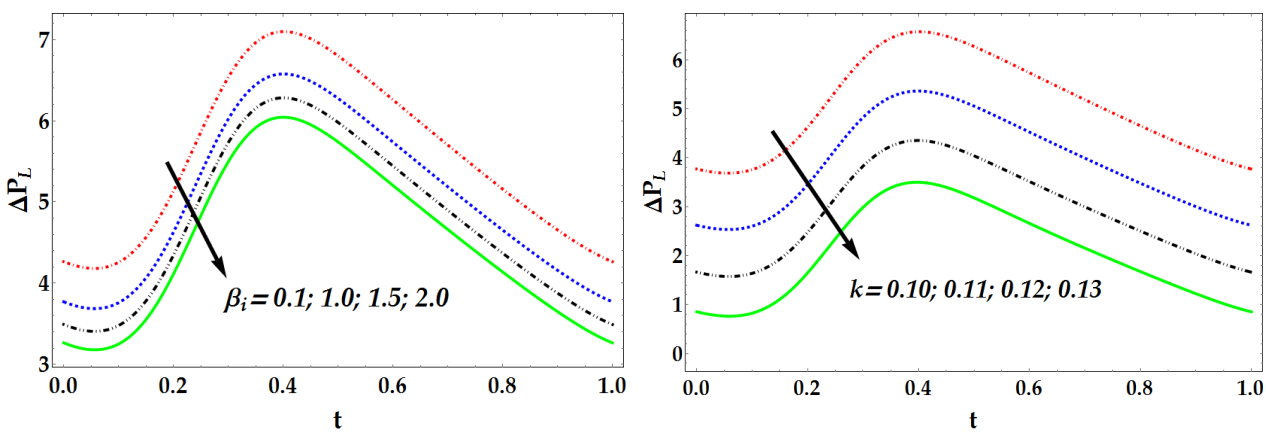

(a) (b)

Fig. 3: Pressure rise for various values of β_i and k. For fixed $(\bar{Q}) = 0.25$, $M = 0.1$, $M = 2$, $\phi = 0.3$, $\beta_i = 1$, $\alpha_1 = 0.3$

5 Conclusion

In this article, Effect of hall and ion slip on peristaltic blood flow in non-uniform porous channel has been studied. The governing flow problem is solved under the approximation of long wave length and low

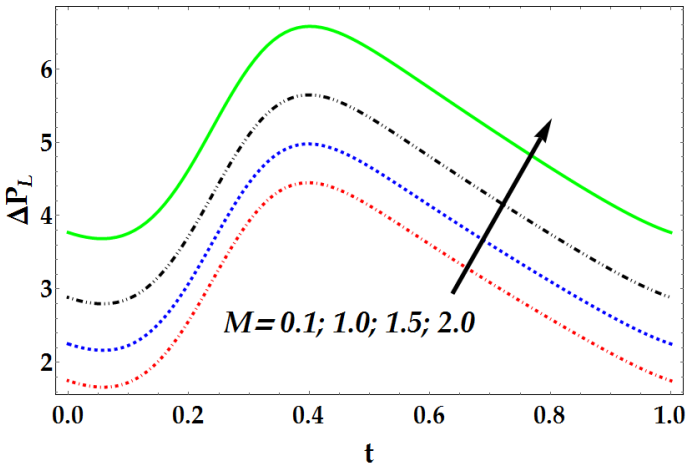

Fig. 4: Pressure rise for various values of M. For fixed $(\bar{Q}) = 0.25$, $\phi = 0.3$, $\alpha_1 = 0.3$, $\beta_i = 1$, $\beta_e = 1$

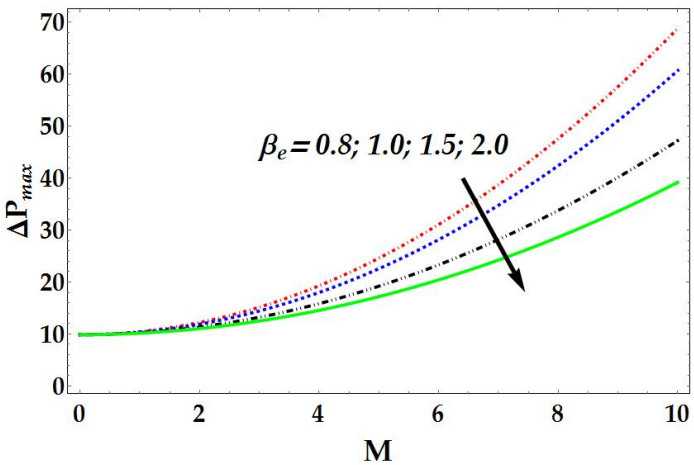

Fig. 5: Maximum pressure rise for various values of β_e. For fixed $\bar{Q} = 0.25$, $\phi = 0.3$, $\alpha_1 = 0.3$, $\beta_i = 1$, $M = 2$

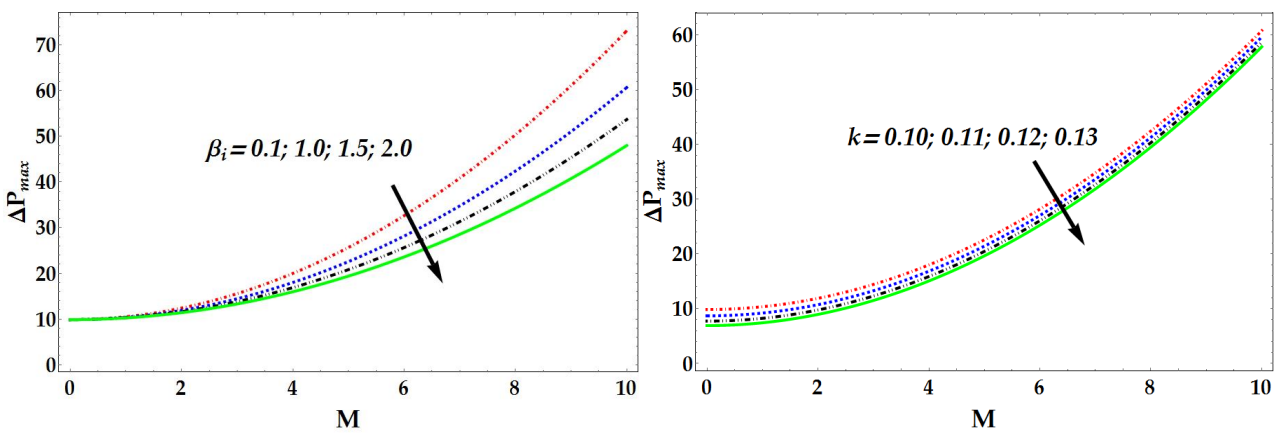

(a) (b)

Fig. 6: Maximum pressure rise for various values of β_i and k. For fixed $\bar{Q} = 0.25$, $M = 0.1$, $M = 2$, $\phi = 0.3$, $\beta_e = 1$, $\alpha_1 = 0.3$

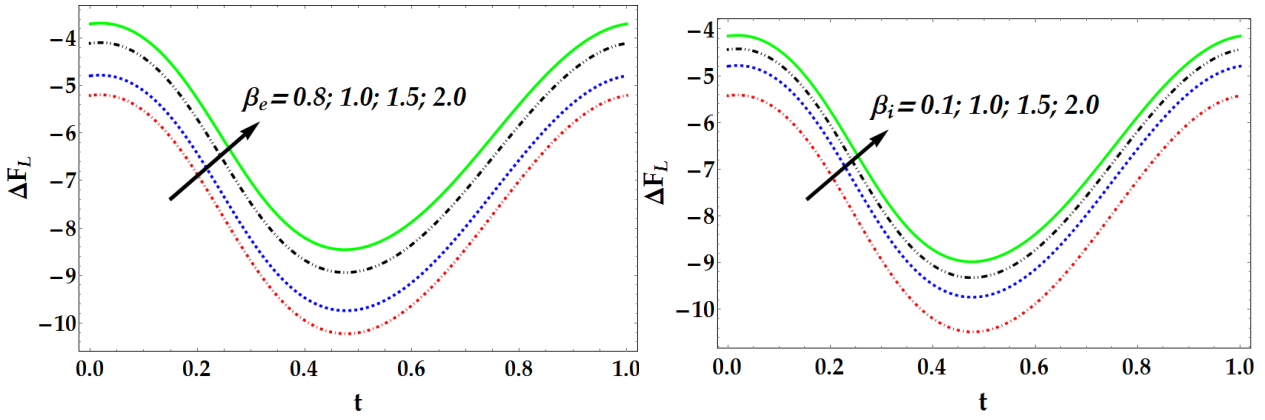

(a) (b)

Fig. 7: Friction force for various values of β_e and β_i. For fixed $(\bar{Q}) = 0.25$, $M = 0.1$, $M = 2$, $\phi = 0.3$, $k = 0.1$, $\alpha_1 = 0.3$

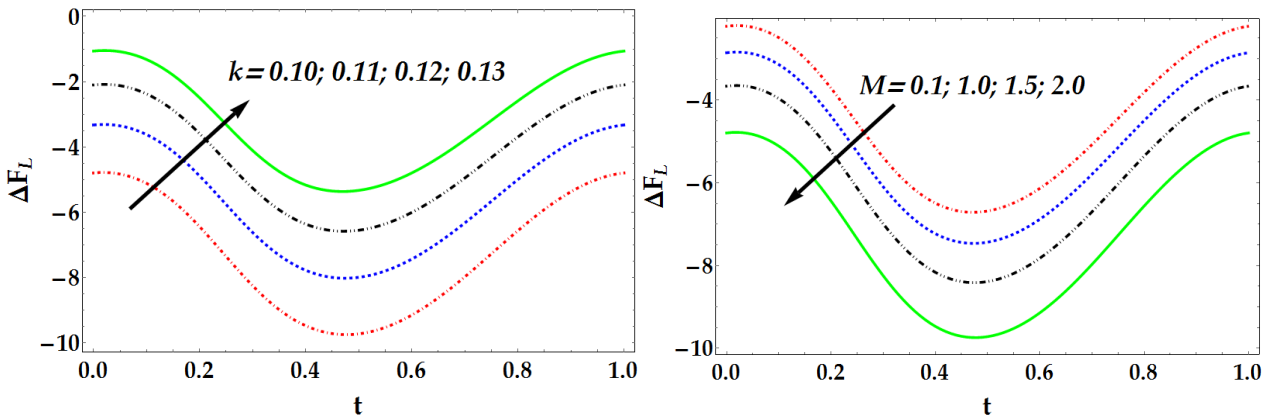

(a) (b)

Fig. 8: Friction force for various values of k and M. For fixed $(\bar{Q}) = 0.25$, $M = 0.1$, $\phi = 0.3$, $\beta_e = 1$, $\beta_i = 1$, $\alpha_1 = 0.3$

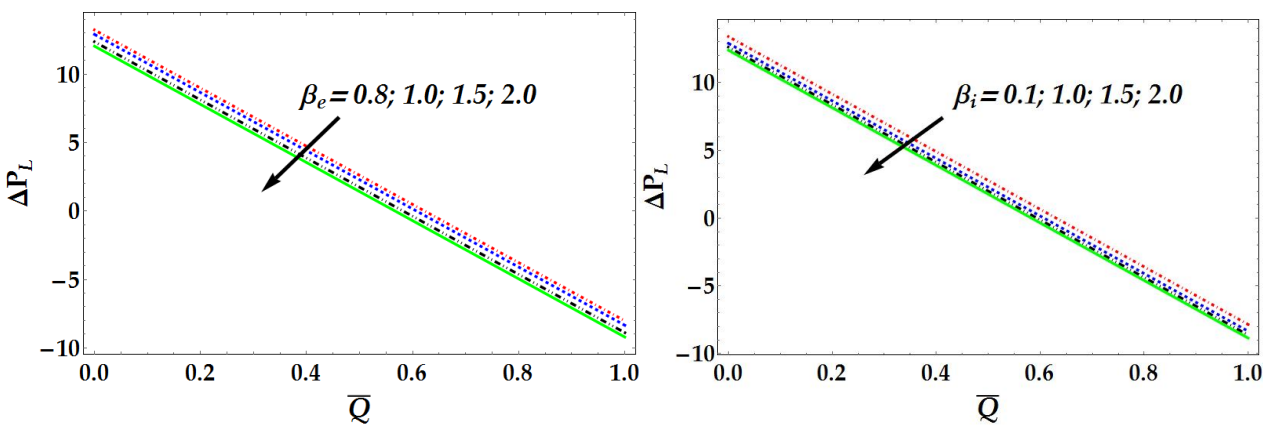

(a) (b)

Fig. 9: Pressure rise vs average volume flow rate for various values of β_e and β_i. For fixed $M = 0.1$, $M = 2$, $\phi = 0.3$, $k = 0.1$, $\beta_i = 1$, $\alpha_1 = 0.3$

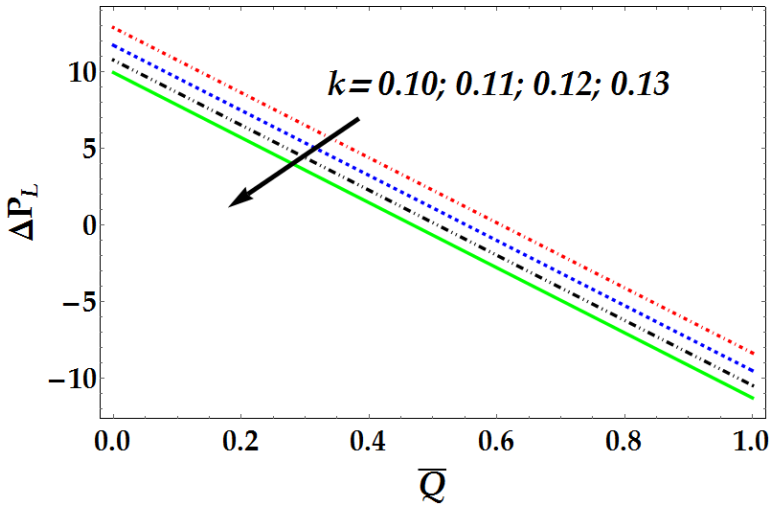

Fig. 10: Pressure rise vs average volume flow rate for various values of k. For fixed $(\bar{Q}) = 0.25$, $M = 0.1$, $M = 2$, $\phi = 0.3$, $\beta_e = 1$, $\alpha_1 = 0.3$

Reynolds number (creeping flow regime). The resulting non-Linear differential equation is solved with the help Homotopy perturbation method and the solution has been obtained up to third order approximation. Numerical computation has been used with the help of computational software "Mathematica" to calculate the expression for pressure rise and friction forces. The main outcomes of this present investigation are described below:

- Pressure rise decreases when β_e, β_i and k increases and its attitude is opposite for friction forces.
- Pressure rise increases for the fluid parameter α_1.
- Maximum pressure rise is also decreasing for β_e, β_i and k.
- Pressure rise for different values of average volume flow rate is also decreasing for β_e, β_i and k.
- Numerical results shows that pressure rise increases when the amplitude of the peristaltic wave increases.
- The present results for a uniform channel can be reduced by taking $\rightarrow 0$.
- It is also observed that the magnitude of the velocity is higher when the fluid depicts non-Newtonian behavior.

References

[1] M. A. Abbas, Y. Q. Bai, et al. Application of drug delivery in magnetohydrodynamics peristaltic blood flow of nanofluid in a non-uniform channel. *Journal of Mechanics in Medicine and Biology* , 2015, **16**: 1650052.

[2] H. Agrawal, B. A. Uddin. Peristaltic flow of blood in a branch. *Ranchi University Mathematics Journal*, 1984, **15**: 111–121.

[3] N. S. Akbar, M. Raza, R. Ellahi. Influence of induced magnetic field and heat flux with the suspension of carbon nanotubes for the peristaltic flow in a permeable channel. *Journal of Magnetism and Magnetic Materials*, 2015, **381**: 405–415.

[4] N. S. Akbar, M. Raza, R. Ellahi. Peristaltic flow with thermal conductivity of H2O+ Cu nanofluid and entropy generation. *Results in Physics*, 2015, **5**: 115–124.

[5] T. Beg, M. M. Rashidi, et al. Differential transform semi- numerical analysis of biofluid-particle suspension flow and heat transfer in non-darcian porous media. *Computer Methods in Biomechanics and Biomedical Engineering*, 2013, **16**: 896–907.

[6] R. Ellahi, M. M. Bhatti, et al. Effects of magnetohydrodynamics on peristaltic flow of jeffrey fluid in a rectangular duct through a porous medium. *Journal of Porous Media*, 2014, **17**: 143–157.

[7] R. Ellahi, X. Wang, M. Hameed. Effects of heat transfer and nonlinear slip on the steady flow of couette fluid by means of chebyshev spectral method. *Zeitschrift f ur Naturforschung A.*, 2104, **69**(1-2): 1–8.

[8] Y. Fung, C. Yih. Peristaltic transport. *Journal of Applied Mechanics*, 1968, **35**: 669– 675.

[9] N. Gad. Effects of hall currents on peristaltic transport with compliant walls. *Applied Mathematics and Computation*, 2014, **235**: 546–554.
[10] B. B. Gupta, V. Seshadri. Peristaltic pumping in non-uniform tubes. *Journal of Biomech*, 1976, **9**: 105–109.
[11] M. S. Kandelousi. Effect of spatially variable magnetic field on ferrofluid flow and heat transfer considering constant heat flux boundary condition. *European Physical Journal Plus*, 2014, **129**(11): 1–12.
[12] M. S. Kandelousi. Kkl correlation for simulation of nanofluid flow and heat transfer in a permeable channel. *Physics Letters A*, 2014, **378**(45): 3331–3339.
[13] J. R. Keltner, S. R. M. SR, et al. Magnetohydrodynamics of blood flows. *Magnetic Resonance in Medicine*, 1990, **16**: 139–149.
[14] A. R. Khaled, K. Vafai. The role of porous media in modelling flow and heat transfer in biological tissues. *International Journal of Heat and Mass Transfer*, 2003, **46**: 4989–5003.
[15] N. A. Khan, S. Aziz, N. A. Khan. Mhd flow of powell eyring fluid over a rotating disk. *Journal of The Taiwan Institute of Chemical Engineers*, 2014, **45**: 2859–2867.
[16] K. S. Mekheimer. Peristaltic flow of blood under effect of a magnetic field in a non-uniform channel. *Applied Mathematics and Computation*, 2004, **153**: 763–777.
[17] K. S. Mekheimer, A. Salem, A. Zaher. Peristaltically induced mhd slip flow in a porous medium due to a surface acoustic wavy wall. *Journal of Egyptian Mathematical Society*, 2014, **22**: 143–151.
[18] S. Mukherjee, M. Maiti. Unsteady convective diffusion in blood flow through a tube. *Chemical Engineering Communications*, 1984, **28**: 99–109.
[19] S. Nadeem, A. Riaz, et al. Heat and mass transfer analysis of peristaltic flow of nanofluid in a vertical rectangular duct by using the optimized series solution and genetic algorithm. *Journal of Computational and Theoretical Nanoscience*, 2014, **11**(4): 1133–1149.
[20] S. Nikolov, S. Stoytchev. A mathematical model of blood flow in an intracranial aneurysm: Analytical and numerical study. *Journal of Mechanics in Medicine and Biology*, 2006, **6**: 137–151.
[21] W. V. Potters, H. A. Marquering, et al. Measuring wall shear stress using velocity-encoded mri. *Current Cardiovascular Imaging Reports*, 2014, **7**: 1–12.
[22] K. Rajagopal, A. S. A, W. Troy. An existence theorem for the flow of a non- newtonian fluid past an infinite porous plate. *International Journal of Non-Linear Mechanics*, 1986, **21**: 279–289.
[23] S. Rashidi, M. Dehghan, et al. Study of stream wise transverse magnetic fluid flow with heat transfer around an obstacle embedded in a porous medium. *Journal of Magnetism and Magnetic Materials*, 2015, **378**: 128–137.
[24] S. Rashidi, A. Nouri-Borujerdi, et al. Stress-jump and continuity interface conditions for a cylinder embedded in a porous medium. *Transport in Porous Media*, 2015, **107**(1): 171–186.
[25] A. Riaz, S. Nadeem. Exact solution for peristaltic flow of jeffrey fluid model in a three dimensional rectangular duct having slip at the walls. *Applied Bionics and Biomechanics*, 2014, **11**(1): 81–90.
[26] A. H. Shapiro, M. Y. Jaffrin, S. L. Weinberg. Peristaltic pumping with long wavelength at low reynolds number. *Journal of Fluid Mechanics*, 1969, **37**: 799–825.
[27] M. Sheikholeslami. Effect of uniform suction on nanofluid flow and heat transfer over a cylinder. *Journal of The Brazilian Society of Mechanical Sciences and Engineering*, 2015, **37**(6): 1623–1633.
[28] M. Sheikholeslami, S. Abelman. Two-phase simulation of nanofluid flow and heat transfer in an annulus in the presence of an axial magnetic field. *IEEE Transactions on Nanotechnology*, 2015, **14**(3): 561–569.
[29] M. Sheikholeslami, H. R. Ashorynejad, et al. Homotopy perturbation method for three-dimensional problem of condensation film on inclined rotating disk. *Scientia Iranica*, 2012, **19**(3): 437–442.
[30] M. Sheikholeslami, H. R. Ashorynejad, P. Rana. Lattice boltzmann simulation of nanofluid heat transfer enhancement and entropy generation. *Journal of Molecular Liquids*, 2016, **214**: 86–95.
[31] M. Sheikholeslami, R. Ellahi, et al. Effects of heat transfer in flow of nanofluids over a permeable stretching wall in a porous medium. *Journal of Computational and Theoretical Nanoscience*, 2014, **11**(2): 486–496.
[32] M. Sheikholeslami, D. D. Ganji. Heat transfer of cu-water nanofluid flow between parallel plates. *Powder Technology*, 2013, **235**: 873–879.
[33] M. Sheikholeslami, D. D. Ganji. Nanofluid flow and heat transfer between parallel plates considering brownian motion using dtm. *Computer Methods in Applied Mechanics and Engineering*, 2015, **283**: 651–663.
[34] M. Sheikholeslami, D. D. Ganji, et al. Analytical investigation of jeffery-hamel flow with high magnetic field and nanoparticle by adomian decomposition method. *Applied Mathematics and Mechanics*, 2012, **33**(1): 25–36.
[35] M. Sheikholeslami, T. Hayat, A. Alsaedi. Mhd free convection of al 2 o 3-water nanofluid considering thermal radiation: A numerical study. *International Journal of Heat and Mass Transfer*, 2016, **96**: 513–524.
[36] M. Sheikholeslami, M. M. Rashidi. Effect of space dependent magnetic field on free convection of fe 3 o 4-water nanofluid. *Journal of The Taiwan Institute of Chemical EngINEERS*, 2015, **56**: 6–15.
[37] M. Sheikholeslami, M. M. Rashidi, et al. Free convection of magnetic nanofluid considering mfd viscosity effect. *Journal of Molecular Liquids*, 2016, **218**: 393–399.

[38] M. Sheikholeslami, K. Vajravelu, M. M. Rashidi. Forced convection heat transfer in a semi annulus under the influence of a variable magnetic field. *International Journal of Heat and Mass Transfer*, 2016, **92**: 339–348.
[39] X. Si, L. Zheng, et al. The effects of slip velocity on a micropolar fluid through a porous channel with expanding or contracting walls. *Computer Methods in Biomechanics and Biomedical Engineering*, 2014, **17**: 423–432.
[40] A. Sinha, J. C. Misra. Mhd flow of blood through a dually stenosed artery: Effects of viscosity variation, variable haematocrit and velocity-slip. *Canadian Journal of Chemical Engineering*, 2014, **92**: 23–31.
[41] S. Srinivas, R. Gayathri. Peristaltic transport of a newtonian fluid in a vertical asymmetric channel with heat transfer and porous medium. *Applied Mathematics and Computation*, 2009, **215**: 215 (2009), pp. 185–196.
[42] L. Srivastava, V. Srivastava, S. Sinha. Peristaltic transport of a physiological fluid. part-i. flow in non-uniform geometry. *Biorheology*, 1982, **20**: 153–166.
[43] L. M. Srivastava, V. P. Srivastava. Peristaltic transport of a power–law fluid: Application to the ductus efferentes of the reproductive tract. *Rheologica Acta*, 1988, **27**: 428–433.
[44] V. Stud, G. Sephon, R. Mishra. Pumping action on blood flow by a magnetic field. *Bulletin of Mathematical Biology*, 1977, **39**: 385–390.
[45] P. Tazraei, A. Riasi, B. Takabi. The influence of the non-newtonian properties of blood on blood-hammer through the posterior cerebral artery. *Mathematical Biosciences*, 2015, **264**: 119–127.
[46] G. Torotra, S. Grabowski. The cardiovascular system: The blood. *Principles of Anatomy and Physiology*, 1993, 566–590.
[47] D. Tripathi. Numerical study on peristaltic transport of fractional bio-fluids. *Journal of Mechanics in Medicine and Biology*, 2011, **11**: 1045–1058.
[48] G. Varshney, V. Katiyar, S. Kumar. Numerical modelling of pulsatile flow of blood through a stenosed tapered artery under periodic body acceleration. *Journal of Mechanics in Medicine and Biology*, 2010, **10**: 251–272.

Appendix

Table 3: Nomenclature

$\tilde{u}, \tilde{v}$	velocity components (m/s)
$\tilde{x}, \tilde{y}$	Cartesian coordinate (m)
$\tilde{p}$	pressure in fixed frame (N/m^2)
$\tilde{a}$	wave amplitude (m)
$b(\tilde{x})$	width of the channel (m)
$\tilde{c}$	wave velocity (m/s)
Re	Reynolds number
$\tilde{t}$	time (s)
q	Embedded parameter
$K(\ll 1)$	constant
A_1	Rivilin Erickson tensor
B	magnetic field (N/mA)
Q	volume flow rate (m^3/s)
B, C	Material parameters
M	Hartman number
S	stress tensor
k	porosity parameter
E	Electric field (V.m^{-1})
V	Fluid velocity (m/s)
j	Current density(A.m^2)

Table 4: Greek Symbols

μ	viscosity of the fluid (N s/m^2)
σ	electrical conductivity (S/m)
δ	wave number (m^{-1})
ν	kinematic viscosity (m^2/s)
λ	wavelength (m)
ϕ	Amplitude ratio
α_1, M	Material parameters
ω_e	cyclotron frequency
τ_e	electron collision time
β_i	Ion slip parameter
β_e	Hall parameter